Robust Fault Detection Filter Design for Commercial Aircraft

Bálint Vanek, Peter Seiler, József Bokor, and Gary J. Balas

Abstract The present article considers the application of robust $\mathscr{H}_\infty$ filters for nonlinear aircraft models in cruise flight conditions. The achieved performance of various design scenarios are first compared with the best achievable lower bound, calculated using frequency-gridding method. The synthesis problem is than validated on the linear uncertain aircraft model, later on the nonlinear, high-fidelity aircraft simulator. The fault isolation and separation properties are compared of different designs based on various model abstraction levels on several candidate fault scenarios.

1 Introduction

Modern fly-by-wire aircraft flight control systems are becoming more complex with many actuators controlling several aerodynamic surfaces. While performance goals, like aerodynamic drag minimization and structural load suppression are becoming more and more important the safety of flight has to be improved as well. In parallel, there is a clear trend towards the All-Electric Aircraft. Recently, Airbus introduced on the A380 a new hydraulics layout, where the three Hydraulics circuitry is replaced by a two Hydraulics plus two Electric layout, which saves one ton mass for the aircraft. Each primary surface has a single hydraulically powered actuator and electrically powered back-up with the exception of the outer aileron, which uses the two hydraulic systems together. Consequently, the trends of complexity and more-electric architectures raise the importance of availability, reliability and operating safety. For safety critical systems, like aircrafts, the consequence of faults in the control system hardware and software can be extremely serious in terms of human mortality and economical impact. Therefore, there is a growing need for on-line supervision and fault diagnosis to increase the reliability of such safety critical systems. The traditional approach to fault diagnosis in the wider application context is based on hardware redundancy methods which use multiple sensors, actuators computers and software to measure and control a particular variable. The interest is in methods which do not require additional hardware redundancy, and only rely on the ever increasing level of computational power onboard the aircraft. In analytical redundancy schemes, the resulting difference generated from the consistency

B. Vanek and J. Bokor are with Systems and Control Laboratory, Computer and Automation Research Institute, Hungarian Academy of Sciences, vanek@sztaki.hu · P. Seiler and G.J. Balas are with the Aerospace and Engineering Mechanics Department, University of Minnesota, seiler@aem.umn.edu

checking of different variables is called as a residual signal. Based on the mathematical model of the plant, analytical relation between different sensor outputs can be used to generate residual signals. The basis for residual generation is analytical redundancy, which according to Chow [7] takes two forms: 1) direct redundancy-the relationship among instantaneous outputs of sensors; and 2) temporal redundancy-the relationship among the histories of sensor outputs and actuator inputs. It is based on these relationships that outputs of (dissimilar) sensors (at different times) can be compared. The residuals resulting from these comparisons are then measures of the discrepancy between the behavior of observed sensor outputs and the behavior that should result under normal conditions. The residual should be zero when the system is normal, and should diverge from zero when a fault occurs in the system. This zero and non-zero property of the residual is used to determine whether or not faults have occurred. Analytical redundancy makes use of a mathematical model and the goal is the determination of faults of a system from the comparison of available system measurements with a priori information represented by the mathematical model, through generation of residual quantities and their analysis. Various approaches have been applied to the residual generation problem, the parity space approach [7], the multiple model method [5], detection filter design using geometric approach [18], frequency domain concepts [11], unknown input observer concept [6], and dynamic inversion based detection [9]. Most of these design approaches refer to LTI systems. The geometric concept is further generalized to LPV systems in [3], while input affine nonlinear systems are considered in [8]. The basic concepts underlying observer-based FDI schemes are the generation of residuals and the use of an optimal or adaptive threshold function to differentiate faults from disturbances, see [10, 12, 19]. Generally, the residuals, also known as diagnostic signals, are generated by the FDI filter from the available input and output measurements of the monitored system. The threshold function is used to robustify the detection of the fault by minimizing the effects from false faults, disturbances and commands on the residuals. For fault isolation, the generated residual has to include enough information to differentiate said fault from another, usually this is accomplished through structured residuals or directional vectors. Robustness of the FDI algorithm is determined by its capability to de-sensitize the filters from disturbances, errors, and unmodelled dynamics. Estimation is important for both signal processing and feedback control and it is the most common approach used in fault detection. The well-known Kalman Filter [15, 14] provides an optimal minimum-variance estimator for linear systems subject to Gaussian noise. The rise of robust control techniques in the 1980s led to an interest in alternative filters, e.g. the $\mathscr{H}_2$ filter (a generalization of the Kalman filter) and the $\mathscr{H}_\infty$ filter ([22]). These methods assume the signals are generated by a known dynamic model and robustness with respect to model uncertainty is an important consideration. Numerous papers on robust filter design have appeared [2, 16, 1, 20]. This paper considers the FDI problem as a robust $\mathscr{H}_\infty$ filtering problem for uncertain, continuous-time systems with the uncertainties described by LTI dynamics. The D-K iteration yields sub-optimal solutions but is a standard method to handle the nonconvexity that arises in robust control synthesis. In robust filter design problem, the filter enters the design interconnection in an open loop (rather than a feedback) configuration and this structure can be exploited. In [20], the filter synthesis problem is converted into a semi-definite program (SDP) using a special IQC factorization to enforce nominal stability. The set of allowable IQC multipliers is, in general, infinite dimensional. The approach in [20] obtains a finite dimensional optimization by restricting the multipliers to be combinations of chosen basis functions. Our aim is to extend the IQC based analysis and filter design developed in [21] to the aircraft example detailed in the present article. The importance of this paper is on the application (simulation) of the D-K iteration based LTI FDI technique to a nonlinear high-fidelity aircraft, where issues of model uncertainty, realistic disturbances and robustness have to be accounted for in the design stage. Three FDI filters are developed based on the linear open-loop aircraft model with the main design goal of detecting, isolating, and identifying faults in the six degrees of freedom motion of the aircraft during closed-loop flight: aileron and elevator actuator faults. These three filters are designed based on three different aircraft

models, using similar interconnection and weights specifically designed for one trim point. The remainder of the paper has the following structure. Section 2 formulates the robust fault detection filter design problem and describes the proposed solution method. The application example of a civil wide-body aircraft is described in Section 3. The method is applied to the high fidelity aircraft example that demonstrates the proposed approach is given in Section 4. Finally, the paper is concluded in Section 5.

2 Robust Fault Diagnosis Problem

This section presents a brief introduction to the main definitions and goals of $\mathscr{H}_\infty/\mu$ fault detection and isolation filters. Figure 2 illustrates the $\mathscr{H}_\infty/\mu$ robust fault diagnosis problem. P is a nominal LTI plant, and F is the desired stable filter. The vectors f,d,u correspond to the fault, disturbance and control inputs respectively. The estimation error, to be minimized, is given by e, and is the difference between the fault and the residual vector, *res*. The output from the plant is given by vector y, and w,z denote the fictitious input and output of the uncertain model, Δ.

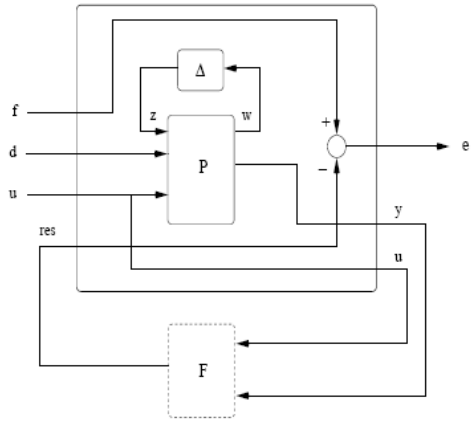

Fig. 1 $\mathscr{H}_\infty/\mu$ filter problem with uncertain model

The state space representation of the linearized plant is given by:

$$\dot{x}(t) = Ax(t) + Bu(t) + B_f f(t) + B_d d(t) + B_\delta z(t) \tag{1}$$

$$y(t) = Cx(t) + Du(t) + D_f f(t) + D_d d(t) + D_\delta z(t) \tag{2}$$

The corresponding diagnostic filter, residual and error signals in case of actuator fault detection are given by:

$$\dot{x}_r(t) = A_r x_r(t) + B1_r u(t) + B2_r y(t) \tag{3}$$

$$res(t) = C_r x_r(t) + D1_r u(t) + D2_r y(t) \tag{4}$$

$$e(t) = Mf(t) - Ires(t) \tag{5}$$

where all matrices are of appropriate dimensions. The perturbation output, z, in Figure 1, can be considered as a special type of disturbance. Combine the disturbance, and the perturbation output, into a generalized disturbance vector, [6], the modified problem can be stated as a standard $\mathscr{H}_\infty$ formulation, Figure 2.

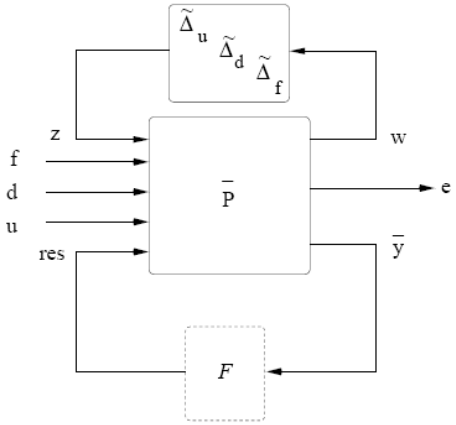

Fig. 2 $\mathscr{H}_\infty/\mu$ interconnection for robust performance assessment

The objective of the $\mathscr{H}_\infty/\mu$ filter synthesis is to find a stable filter that minimizes the transfer function from the disturbances to the errors (i.e min $||TF_{e\underline{\hat{d}}}||$ while maximizing the faults effect on the errors (i.e. max $||TF_{ef}||$) where $\hat{d} = [du]$ is the generalized disturbance, see [19], while considering the effects of structured uncertainty. The present problem formulation uses input uncertainty to describe the discrepancy between the nominal model and the behavior of the nonlinear model around the trim point. Since the flight control surfaces, and hence the control inputs, are structured into several groups, the uncertainty description has similar structure as well. It is also assumed that only LTI uncertainties are present, then the filtering problem reduces to the μ synthesis problem.

3 Aircraft Model

3.1 General Aircraft Characteristics

The aircraft model used in this paper is a wide-body aircraft from Airbus. The aircraft has two engines and a nominal weight of 200 tons. Some of its performance at cruise condition are cruising speed of 240 knots altitude of 30000 ft. The aircraft has 19 control inputs, and measurement of 6-DOF motion with load factor (n_x, n_y, n_z), body rate (p, q, r), velocity (V_T), aerodynamic angles (α, β), position (X, Y, Z) and attitude (ϕ, θ, ψ) outputs. The inputs are: $pi1$ left and $pi2$ right engine; AF (airbrake), which is disabled at cruise flight condition, $\delta_{a,IL}$ Aileron internal Left; $\delta_{a,IR}$ Aileron internal Right; $\delta_{a,EL}$ Ail external Left; $\delta_{a,ER}$ Ail external Right; $\delta_{sp,1L}$ Spoiler 1 Left; Spoiler 1R; Spoiler 23L; Spoiler 23R; Spoiler 45L; Spoiler

45R; Spoiler 6L; Spoiler 6R; $\delta_{e,L}$ Elevator Left; $\delta_{e,R}$ Elevator Right; δ_r Rudder; and δ_{ih} Trimmable Horizontal Stabilizer which is used for trimming purposes.

The aerodynamic data is high-fidelity and propriety of Airbus S.A.S. The rigid body aircraft equations of motion are augmented with actuator and sensor characteristics, detailed in [13]. The nonlinear body-axes rigid body dynamics includes 13 states using quaternion formalism: p,q,r body rates, u,v,w velocities all in body axes, q_0,q_1,q_2,q_3 quaternions, representing the rotation between the body and inertial axes, and X,Y,Z positions in the North-East-Down coordinate frame, assuming Flat Earth for simplicity.

3.2 Linearized Aircraft Model

In the present article one design point, cruise flight condition, is considered. The LTI model of the aircraft is obtained at level flight, with $p = q = r = 0$ rad/s, $v_x = 194.36$ m/s, $v_y = 0m/s$, $v_z = 15.13$ m/s, at 9144 m altitude. Since the original aircraft model uses quaternions, which impose additional constraints on the state equations, the model used for trim and linearization is rewritten using conventional Euler angles [23]. The model used for trim is an open-loop model without the control loop and, since the actuators and sensors are assumed to have unit dc gain and low-pass characteristics, their dynamics is omitted. Trim is obtained with zero aileron, rudder and elevator deflection, left and right engines are providing the same amount of thrust to balance the yawing motion. Pitch axis trim is obtained with the Trimmable Horizontal Stabilizer, while the aircraft has 2.66 degrees Angle-of-attack. The resulting 12 state linear model is unstable. The airbrake, which is disabled at high Mach numbers, is removed from the control inputs since it has no effect on the aircraft.

3.3 Model Reduction for FDI

The open loop aircraft model is slightly unstable around the yaw angle (ψ), and has two modes (X,Y) which are integrators. Since the FDI problem is invariant of X,Y positions and yaw angle these states are removed from the dynamics. The resulting model with nine states, as shown on Figure 3, almost perfectly matches the original 12 states model in the behavior of the remaining states, and outputs. The resulting system with nine states is stable which is necessary to linear estimator based FDI techniques. The resulting LTI model is augmented with first order sensor and actuator dynamics, to account for their effect on the aircraft behavior. Hence, the filters designed based on the reduced model are most likely to be applicable to the original model and to the nonlinear aircraft dynamics.

4 FDI Filter Design for the Aircraft

First, the formulation of the filtering problem and designing the weights are presented. Detailed simulations on the high-fidelity aircraft model with aileron and elevator faults injected follows.

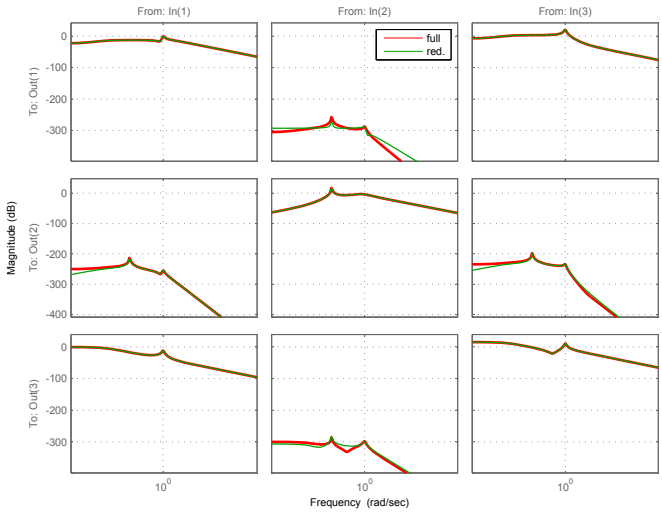

Fig. 3 Aileron, elevator and rudder to p,q, and r Bode diagram of full and reduced LTI model

4.1 Filter Design Steps

The main idea behind the filter design formulation in this article is that of model matching with tracking [17], which results in detection and isolation on the FDI filter output. As seen on Figure 4, the objective is to minimize the error (e) between the fictitious fault input (f) and the residual (res), which is the output of the FDI filter. The filter must be able to detect and isolate aileron and elevator actuator faults (similar to a decoupled tracking problem from a control point of view) while rejecting disturbances and noise and being robust to model uncertainties. Since the FDI design

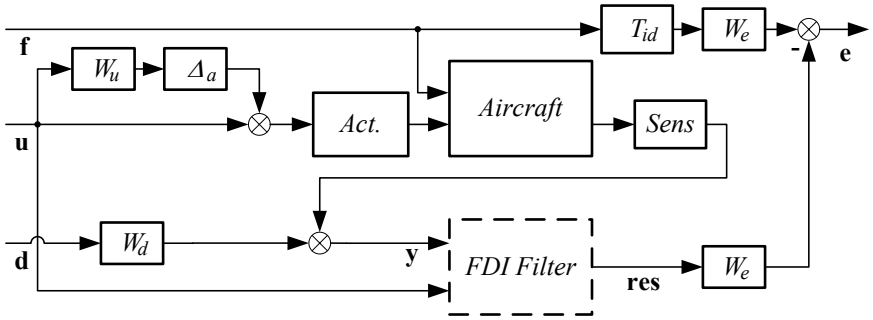

Fig. 4 FDI filter design weighted interconnection

results in a rather large filter, with 30 inputs (y has 12 measurements and the 18 control inputs are also fed to it) and two outputs (res_{ail}, res_{ely}), an alternate approach is also investigated with decoupled aileron and elevator fault detection, using reduced models. The blocks in the filter design interconnection correspond to weight-

ing functions, design specifications and system components. Model mismatches are accounted for as weighted unmodeled LTI dynamics, W_u is diagonal, where $W_u = diag < w_1, w_1, w_3, w_3, w_3, w_3, w_2, w_2, w_2, w_2, w_2, w_2, w_2, w_3, w_3, w_4, w_3 >$ corresponds to different levels of uncertainty on engines w_1, ailerons, elevators, rudder w_3, spoilers w_2, and trimmable horizontal stabilizer w_4. Each of the have approximately 10% uncertainty at low frequency and higher than 100% at high frequencies, the difference between them is their frequency characteristics. Engines and THS have slower dynamics, after their bandwidth their uncertainty grows to 100% after slightly after their cutoff frequency. Similarly the other actuators of aerodynamic surfaces have high uncertainty after their bandwidth, but since their time constants are lower their uncertainty grows below 100% at higher frequencies. The structured input uncertainty block Δ_a is grouped according to the actuator functional groups: $\Delta_a = diag < \Delta^{2\times2}_{engine}, \Delta^{4\times4}_{aileron}, \Delta^{8\times8}_{spoiler}, \Delta^{3\times3}_{longitudinal}, \Delta^{1\times1}_{rudder} >$. Disturbances are modeled as exogenous signals, since all signals are normalized in the $\mathscr{H}_\infty$ framework W_d weight is used to scale the noise level on sensors, which is assumed to have, depending the dimension of the signals, $0.5deg, 0.5deg/s, 0.01m/s, 0.1m/s^2, 0.03m$ magnitude noise on all channels. The ideal fault response signal is a low-pass filtered version of f. Two different choices are investigated in the article, one is with 1 *sec* time constant ($T^1_{id} = \frac{1}{s^2+2s+1}$ the other with 0.1 *sec* time constant ($T^2_{id} = \frac{100}{s^2+20s+100}$ to understand the tradeoffs between detection time, false alarm rate and missed detections in the presence of uncertainties. The error between the ideal fault response and the filter residual is weighted with $W_e = \frac{2s+20}{5s+5} I_{2\times2}$ which requires good fault detection performance in the low frequency range until $1rad/s$ and weights less the higher frequency content, while the diagonal structure enforces the isolation property of the filter. The weights used in the system interconnection (Figure 4) are derived from the design objectives. Finally, the system model is composed of actuator dynamics: $Act = diag < act_{engine} I_{2\times2}, act_{aileron} I_{4\times4}, act_{spoiler} I_{8\times8}, act_{elevator} I_{2\times2}, act_{rudder}, act_{THS} >$,sensor dynamics:$Sens =< sens_{rate} I_{3\times3}, sens_{angle} I_{2\times2}, sens_{velocity}, sens_\theta, sens_\phi, sens_{acc} I_{3\times3}, sens_Z >$, and rigid body dynamics, denoted as *Aircraft*. The corresponding values are Airbus propriety, hence they are not discusses here.

As mentioned earlier, two design choices are made when selecting the aircraft model. One detailed on Figure 4 considers the full 6-DOF aircraft dynamics, which results in a rather large filter. The other, a with a slightly different interconnection, considers the aileron and the elevator fault detection problems separately. In the aileron FDI problem the aircraft has only 15 inputs, since the elevators and THS does not affect the lateral dynamics, where the aileron actuator has influence. Moreover, measurement of $q, \alpha, V, \theta, a_x, a_z, Z$ has no influence on the aileron FDI problem and with the remaining inputs and outputs the aircraft dynamics can be simplified from nine to four states. Similar can be done with the elevator FDI problem, where aileron and rudder inputs and p, r, β, ϕ, a_y outputs are unnecessary and the longitudinal model only has 5 states.

The FDI filter synthesis is based on the D-K iteration, which unlike the standard $\mathscr{H}_\infty$ synthesis takes into account the structure of the uncertainty block Δ_a. Moreover state-of-art software packages exist [4] for the solution as a part of MATLAB. In parallel with the D-K iteration based μ-synthesis results, for each filter design setup, the $\mathscr{H}_\infty$ solution is also calculated, which usually results better conditioned filters with lower state numbers.

4.2 Analysis and Results

A lower bound on the optimal performance was computed using frequency-gridding method described in [21]. The frequency grid consisted of 25 logarithmically spaced

points between 0.01 and $100 rad/sec$. Figure 5 shows the lower bounds versus frequency. The largest value across frequency is 0.12 of the ideal optimal case, $\mathscr{H}_\infty$ synthesis achieved 1.64 in the lower frequency range, while the D-K synthesis achieved peek gain value of 0.64 which corresponds to higher performance.

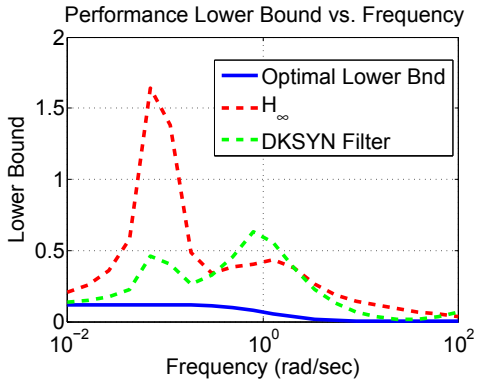

Fig. 5 Theoretical lower bound and achieved lower bounds of the FDI problem formulation

The filters are applied to the nonlinear aircraft model after taking the trim values into consideration, on both control input and sensor output signals. Since the simulation is implemented under SIMULINK with $0.01 sec$ fixed step size, the corresponding filters are also discretized with the same sampling time using bilinear transformation. It is also worth mentioning, that the simulation is in closed-loop with the flight control system set to altitude and heading hold mode and moderate atmospheric windgust disturbances are perturbing the aircraft flight.

The first fault scenario is left inboard aileron liquid jamming as seen on Figure 6, this means that a bias occurs on the rod sensor and the actuator shifts from it nominal $1.5 deg$ deflection to $-0.75 deg$ deflection and it remains $-2.25 deg$ apart from it commanded position.

Figure 6 also shows the abrupt change in roll rate at $10 sec$ when the fault occurs, otherwise slight deflection can be seen on the rudder but elevator and THS is unaffected, mainly the right aileron compensates the effect of the failure.

First the μ filter with $1 sec$ time constant on the ideal fault response is applied to the problem, as shown on Figure 7 the coupled and the decoupled filter also detects the fault and reaches an approximate steady state value after $10 sec$, although the bias on the actuator is $-2.25 deg$ the estimate is between $-0.1 rad$ to $-0.175 rad$ which is at least $5.7 deg$. The isolation property of both coupled and de-coupled filters can be seen, as the elevator fault signal is nearly identical to zero.

The following scenario is the μ filter with $0.1 sec$ time constant, which provides also excellent detection and isolation properties. As seen on Figure 8 the filters reach steady state after $7.5 sec$ which is not significantly faster than with the previous design with $1 sec$ time constant. It is found during the filter synthesis that further decreasing the ideal response time constant does not improve the performance and only performance degradation occurs with further increasing the response speed.

To show the efficiency of the D-K iteration based design a $\mathscr{H}_\infty$ filter with with $0.1 sec$ time constant is also synthesized. As shown on Figure 9 the decoupled filter achieves significantly lower steady state value, making the detection thresholding difficult, while the coupled design does not satisfy the isolation property, since large signals can be seen on the otherwise healthy elevator actuator.

The second scenario is elevator runaway. At $10 sec$ the elevator drifts away from its current position with $1 deg/s$ rate. According to the specification runaway has

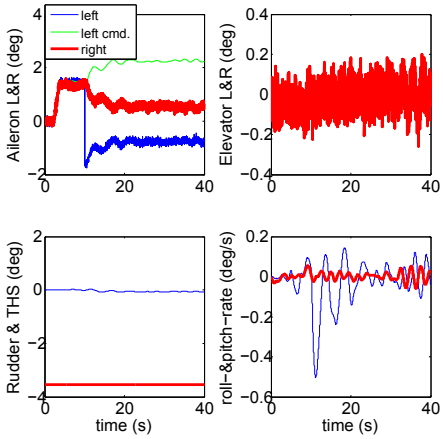

Fig. 6 Aileron liquid jamming scenario, fault occurs at 10*s*

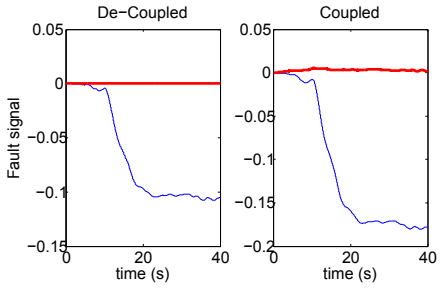

Fig. 7 Aileron liquid jamming scenario, μ filter with 1*sec* time constant

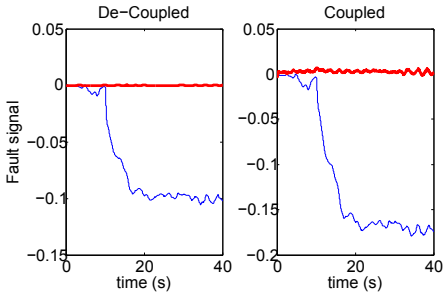

Fig. 8 Aileron liquid jamming scenario, μ filter with 0.1*sec* time constant

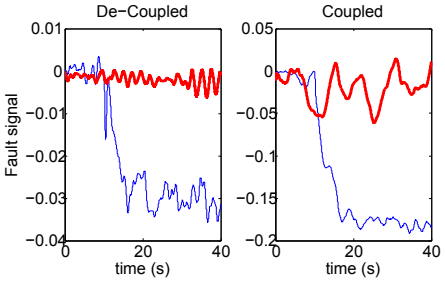

Fig. 9 Aileron liquid jamming scenario, $\mathscr{H}_\infty$ filter with 0.1*sec* time constant

to be detected before 2.5*deg*, meaning there is 2.5*sec* for detection in this case. As shown on Figure 10 the elevator runaway results initially in small pitch rate. But later, around 25*sec*, as the aircraft drifts away from the trim condition, the control system starts to counteract radically using high elevator commands which causes large pitch rate and oscillatory motion. The THS is also deflected to counteract the elevator deflection, but roll rate and rudder command remains unaffected.

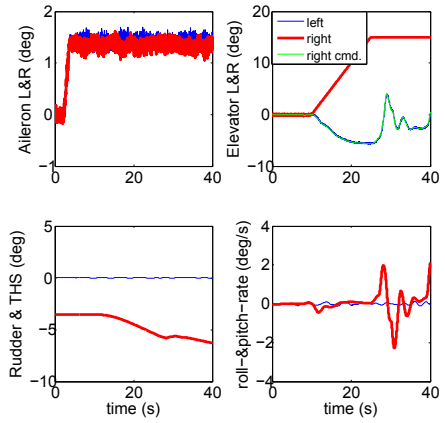

Fig. 10 Elevator runaway scenario, fault occurs at 10*s* with $1deg/s$ rate

The μ filter with 1*sec* time constant on the ideal fault response is applied to the second scenario, as shown on Figure 11. The coupled filter detects the runaway and indicates the fault after few seconds given the threshold is around 0.1, which provides safe false alarm protection in other fault cases. On the other hand the de-coupled filter does not indicate the fault and remains unaffected, indicating the necessity of coupled synthesis.

The μ filter with 0.1*sec* time constant on the ideal fault response is applied next to the second scenario, as shown on Figure 12. The de-coupled filter still does not work as expected. The coupled filter provides similar response to the previous scenario, the difference in time constant cannot be seen, due to the characteristics of the fault and the fact that only little margin is left to increase the speed of response of the detection filter with the current approach, with given weights. It is worth men-

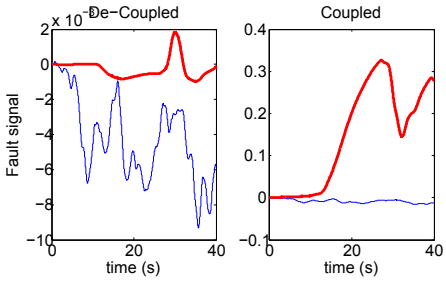

Fig. 11 Elevator runaway, μ filter with 1*sec* time constant

tioning here, that due to the cruise flight condition, where little elevator excitation is expected, the case when the elevator is stuck is difficult to detect.

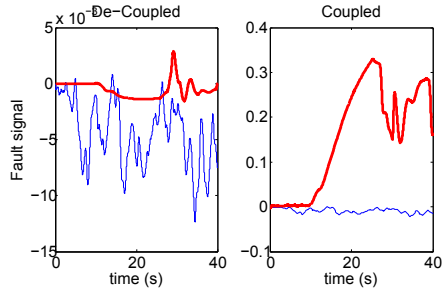

Fig. 12 Elevator runaway, μ filter with 0.1*sec* time constant

5 Conclusions

This paper considered the design of robust $\mathscr{H}_\infty/\mu$ filters and their application to a high fidelity aircraft model, and shows the advantages of advanced methods, those are candidates for future industrial implementation. Aileron and elevator faults are successfully detected and when designed properly isolated from each other in reasonable time. Performance of different designs with faster and slower ideal fault detection response are compared and the article shows the performance bounds on detection speed, given the present model and methods. It is also shown that elevator fault detection is only possible with coupled design taking the full 6-DOF aircraft dynamics into account. Further research should extend the validity of the present approach and based on the present findings provide a fault detection approach for a larger flight envelope.

6 Acknowledgments

This work is supported by the ADDSAFE (Advanced Fault Diagnosis for Safer Flight Guidance and Control) EU FP7 project, Grant Agreement: 233815, Coordinator: Dr. Andrés Marcos.

This material is based upon work supported by the National Science Foundation under Grant No. 0931931 entitled "CPS: Embedded Fault Detection for Low-Cost, Safety-Critical Systems". Any opinions, findings, and conclusions or recommendations expressed in this material are those of the author(s) and do not necessarily reflect the views of the National Science Foundation.

References

1.
2. B. Appleby, J. Dowdle, and W. VanderVelde. Robust estimator design using μ synthesis. In *Proc. of the IEEE Conference on Decision and Control*, pages 640–645, 1991.
3. G. Balas, J. Bokor, and Z. Szabo. Invariant subspaces for LPV systems and their applications. *IEEE Transactions on Automatic Control*, 48(11):2065–2069, 2003.
4. G.J. Balas, A.K. Packard, M.G. Safonov, and R.Y. Chiang. Next generation of tools for robust control. In *Proc. American Control Conf.*, 2004.
5. C. B. Chang and M. Athans. State estimation for discrete systems with switching parameters. *IEEE Transactions on Aerospace and Electronic Systems*, 14:418–425, 1978.
6. J. Chen and R. J. Patton. *Robust Model-based Fault Diagnosis for Dynamic Systems*. Kluwer Academic. Boston., 1999.
7. E.Y. Chow and A.S. Willsky. Analytical redundancy and the design of robust failure detection systems. *IEEE Trans. on Automatic Control*, 29(7):603–614, 1984.
8. C. De Persis, R. De Santis, and A. Isidori. Nonlinear actuator fault detection and isolation for a VTOL aircraft. In *Proceedings of the 2001 American Control Conference, Vols 1-6*, pages 4449–4454, 2001.
9. A. Edelmayer, J. Bokor, and Z. Szabo. A geometric view on inversion-based detection filter design in nonlinear systems. In *Proceedings of the 5th IFAC symposium on fault detection, supervision and safety of technical processes. SAFEPROCESS 2003, Washington*, pages 783–788, Washington, 2003.
10. P.M Frank. Fault diagnosis in dynamic systems using analytical and knowledge-based redundancy - a survey and some new results. *Automatica*, 26:459–474, 1990.
11. P.M. Frank. Online Fault-Detection in Uncertain Nonlinear Systems Using Diagnostic Observers - A Survay. *International Journal of Systems Science*, 25(12):2129–2154, 1994.
12. S.X. Ding Frank, P.M. and B. Köppen-Seliger. Current developments in the theory of FDI. In A. Edelmayer, editor, *Proc. 4th IFAC Symp. on Fault Detection, Supervision and Safety for Technical Processes, Safeprocess'00, Budapest, Hungary.*, pages 16–27, 2000.
13. Philippe Goupil. Oscillatory failure case detection in the a380 electrical flight control system by analytical redundancy. *Control Engineering Practice*, 18:1110–1119, 2009.
14. T. Kailath, A.H. Sayed, and B. Hassibi. *Linear Estimation*. Prentice-Hall, 2000.
15. R.E. Kalman and R.S. Bucy. New results in linear filtering and prediction theory. *Trans. ASME, Ser D., Journal of Basic Engineering*, 83, 1961.
16. R.S. Mangoubi. *Robust Estimation and Failure Detection For Linear Systems*. PhD thesis, Massachusetts Institute of Technology, 1995.
17. A. Marcos, Ganguli S., and Balas G. J. An application of $\mathscr{H}_\infty$ fault detection and isolation to a transport aircraft. *Control Engineering Practice*, 13(1):105–119, 2005.
18. M.A. Massoumnia. A geometric approach to the synthesys of failure detection filters. *IEEE Transactions on Automatic Control*, 31:839–846, 1986.
19. R. J. Patton and J. Chen. Robust fault detection and isolation FDI systems. *Contr. Dynamic Syst.*, 74:176–224, 1996.
20. C.W. Scherer and I.E. Köse. Robust H_2 estimation with dynamic IQCs: A convex solution. In *Proc. of the IEEE Conference on Decision and Control*, pages 4746–4751, 2006.
21. P. Seiler, B. Vanek, J. Bokor, and G. J. Balas. Robust $\mathscr{H}_\infty$ filter design using frequency gridding. In *to apper in: American Control Conference*, 2011.
22. U. Shaked and Y. Theodor. H_∞-optimal estimation: A tutorial. In *Proc. of the IEEE Conference on Decision and Control*, pages 2278–2286, 1991.
23. Robert F. Stengel. *Flight Dynamics*. Princeton University Press, 2004.